# Enhancing Oil Recovery with Hydrophilic Polymer-Coated Silica Nanoparticles

**Alberto Bila [1,2,*]** and **Ole Torsæter [3]**

[1] Department of Chemical Engineering, Faculty of Engineering, Eduardo Mondlane University (EMU), 257 Maputo, Mozambique

[2] Centre of Studies in Oil and Gas Engineering and Technology, Eduardo Mondlane University (EMU), 257 Maputo, Mozambique

[3] PoreLab Research Centre, Department of Geoscience and Petroleum, Norwegian University of Science and Technology (NTNU), 7031 Trondheim, Norway; ole.torsater@ntnu.no

* Correspondence: alberto.bila@uemep.uem.mz

**Abstract:** Nanoparticles (NPs) have been proposed for enhanced oil recovery (EOR). The research has demonstrated marvelous effort to realize the mechanisms of nanoparticles EOR. Nevertheless, gaps still exist in terms of understanding the nanoparticles-driven interactions occurring at fluids and fluid–rock interfaces. Surface-active polymers or other surface additive materials (e.g., surfactants) have shown to be effective in aiding the dispersion stability of NPs, stabilizing emulsions, and reducing the trapping or retention of NPs in porous media. These pre-requisites, together with the interfacial chemistry between the NPs and the reservoir and its constituents, can result in an improved sweep efficiency. This paper investigates four types of polymer-coated silica NPs for the recovery of oil from water-wet Berea sandstones. A series of flooding experiments was carried out with NPs dispersed at 0.1 wt.% in seawater in secondary and tertiary oil recovery modes at ambient conditions. The dynamic interactions of fluids, fluid–rock, and the transport behavior of injected fluid in the presence of NPs were, respectively, studied by interfacial tension (IFT), spontaneous imbibition tests, and a differential pressure analysis. Core flooding results showed an increase in oil recovery up to 14.8% with secondary nanofluid injection compared to 39.7% of the original oil in place (OOIP) from the conventional waterflood. In tertiary mode, nanofluids increased oil recovery up to 9.2% of the OOIP. It was found that no single mechanism could account for the EOR effect with the application of nanoparticles. Instead, the mobilization of oil seemed to occur through a combination of reduced oil/water IFT, change in the rock surface roughness and wettability, and microscopic flow diversion due to clogging of the pores.

**Keywords:** polymer-coated nanoparticles; crude oil recovery; interfacial tension; wettability alteration; flow diversion

## 1. Introduction

Oil companies are facing a decline in production rates due to reduced efficiency in oil recovery from the technologies used today. Technologies such as thermal recovery and injection of chemicals are also hampered by the high costs of preparing and transporting fluids, especially to offshore fields. Furthermore, the discoveries of new oil fields have been scarce [1,2] and/or require more intricate technologies for the production and maximization of crude oil recovery [3]. On the other hand, small pores of the reservoir or thief zones are responsible for trapping a significant amount of residual, making the oil recovery techniques currently used inefficient. Furthermore, injected fluids are trapped in thief zones, which reduces the reservoir's permeability and increases the economics

of oil recovery flooding operations [4]. The use of nanotechnology in the oil and gas industry has been able to improve the oil recovery factor on a laboratory scale. The nanoparticle technology has also proven to be a solution to some of the unsolved problems by old techniques in the upstream oil industry. Nanoparticles are materials with size ranging from 1 to 100 nm in diameter. In addition to size, parameters such as the shape and surface characteristics are key reasons behind the enormous EOR potential of nanoparticles. Owing to their nanoscale size and shape, NPs can improve the flooding potential of the oil recovery fluid through the porous media with little effect on reservoir permeability and increase the recovery efficiency from thief zones [1,3,5]. With reduced size, NPs have a large surface area and, therefore, a large contact area in the swept areas [3]. The interfacial chemical reactivity is increased in the pores of the reservoir in contact with the nanoparticles. Thus, the likelihood of NPs altering the properties of the flowing fluids and rocks to the most favorable conditions for oil recovery can be met. Silica NPs are the most researched nanomaterials to improve the microscopic sweep efficiency of oil recovery drive fluid by changing the interfacial tension and reservoir wettability. The widespread use of silica NPs lies in their natural occurrence in sandstone formations in the form of quartz. In addition, silica NPs can be synthesized with some degree of ease, with manipulated properties, or tailored with different surface coating materials for the desired applications, such as for oil recovery [5–7].

Bera and Belhaj [8] pointed out that 5 to 15% of the OOIP can be achieved with the application of NPs on a laboratory scale. A recent statistical research on nanoparticle core flooding data conducted by Ding et al. [9] showed that the increment in oil recovery can be as high as 30% of the OOIP with NPs injection, but the most frequent range is 5% of the OOIP. Despite promising recoveries, the major challenge remains the formulation of stable nanoparticle dispersion, especially for oil recovery in harsh reservoir environments, of high pressure, high temperature, and high salinity (particularly when divalent ions are present) [10,11].

The functionalization or coating of the surface layer of the particle with polymer chains or other surface additive materials is a novel active area of scientific research; the technique has been desired for improving dispersion stability, for the stabilization of emulsions, to decrease the trapping or retention of NPs in porous media, and to improve the transport of NPs through reservoir pore channels, fundamental pre-requisites for nanoparticle oil recovery process. Omran et al. [12] studied the potential of polymer-coated silica NPs to improve sweep efficiency on a micro-scale. Their study showed that NPs performed more efficiently in water-wet glass micromodels than in intermediate and oil-wet rock models. The displacement efficiency was attributed to the ability of NPs to promote better clusterization of oil, thus leaving small and less connected oil drops trapped in the pores of the micromodel [12]. Saigal et al. [13] reported that silica NPs covalently grafted with polymer chains (2-(dimethylamino)ethyl methacrylate) were extremely efficient emulsifier agents at low concentrations. Qi et al. [14] applied interfacially active, pH-responsive polymer-coated silica NPs for increasing oil production. The authors found that NPs can significantly stabilize heavy oil-in-water emulsions and increase recovery by 10 wt.% of the heavy oil-in-place at concentrations of NPs as low as 0.1 wt.%.

Ponnapati et al. [15] reported an incremental recovery of 7.9% of the OOIP by injecting a stable suspension of polymer-functionalized silica NPs in Berea sandstone. Hendraningrat and Torsæter [13] used a water-soluble polymer, polyvinylpyrrolidone (PVP), to stabilize silica-based nanofluids and attained an increment of 2% of the OOIP. More recently, a series of flooding experiments using polymer-coated silica NPs dispersed in seawater to 0.1 wt.% was carried out by Bila et al. [16] and Bila et al. [17]. The authors reported an increase in oil recovery of about 14% of the OOIP in water-wet Berea core plugs and 5% of the OOIP in neutral-wet cores, respectively.

Following advances in oil recovery, studies have demonstrated marvelous effort to understand the mechanisms associated with NPs injection and their interactions with oil field constituents in order to explain the EOR effect. Wettability alteration to an increasingly water-wet state and reduction in interfacial tension (IFT) have been the two most accepted mechanisms of nanoparticles [9,18]. Interfacial tension and wettability are the most important physical properties that characterize

fluid–fluid and fluid–rock interfaces, respectively. Both properties control the distribution and mobility of reservoir fluids within pore spaces. In oil displacement processes by nanofluid flooding, interfacial tension is expected to decrease during the partitioning of NPs at the oil/water interface from the aqueous solution; this process is governed by the size and wettability of the nanoparticles [19,20]. On the other hand, NPs can adhere to the rock surface because of the attractive forces originating from dipole–dipole interactions [21,22] and/or driven by physical interactions due to the external forces. This process results in the change of the rock surface roughness. A synergistic interaction effect of IFT reduction and wettability alteration creates unfavorable conditions for the oil to reside within pores and promotes its mobilization to the production wells. Additional oil displacement mechanisms are also supposed to be functioning during the nanoparticle EOR process. This includes (i) the creation and stabilization of emulsions [23–25], (ii) structural disjoining pressure [26,27], and (iii) fluid flow diversion, at the microscopic level, due to clogging of the pores [28–31]. Despite these advances/knowledge, gaps still exist in terms of understanding the EOR effect of different types of NPs, including their binding effect with surface additive materials and the resulting interactions with the oil reservoir and its constituents, which act as propellants for oil mobilization, increasing oil recovery. From the various research works, it seems that no single mechanism of nanoparticle EOR can be adopted for all types of formations due to their variable characteristics, such as different types of rock and mineralogy and composition of reservoir fluids. Therefore, despite the widespread use of nanotechnology, a large-scale field application of NPs in the oil and gas industry has not been reported, except for some small-scale field trials [21]. Obviously, this calls for more studies to expand the knowledge of nanotechnology so that it can be applied with less risk in the oil industry. This work demonstrates the applicability of polymer-coated silica NPs for the recovery of crude oil and proposes potential oil displacement mechanisms of nanoparticles.

## 2. Materials and Methods

### 2.1. Silica Nanoparticles and Injection Seawater

Four types of nanostructured particles stabilized by methacrylate-based polymer molecules were used in this work. The polymer shells attached to the particle surface were intended to decrease the hydrophilic nature of the surfaces of silica particles. The nanostructured particles were mainly composed of silicon dioxide ($SiO_2$), aluminum dioxide ($Al_2O_3$), and mixed oxides (MOX). They were spherical and amorphous silica products marketed under the AEROSIL® trade name from Evonik Industries. The particles were supplied to us, for EOR testing, as special research and development (R&D) products, AERODISP®, which are AEROSIL® particles in liquid solution. The properties of NPs as concentrated solutions, as provided by the manufacturer, are given in Table 1. The size of the particles was characterized by the dynamic light scattering technique and varied from 32 to 218 nm in diameter. The concentrated solutions were diluted with synthetic seawater to 0.1 wt.% and used in all tests. To prevent aggregation/agglomeration and ensure homogeneous dispersion, the nanofluids were stirred using a magnetic stirrer for at least 30 min, and immediately injected into the core plugs. Our previous work showed that the nanofluids are stable at room conditions for months [17].

**Table 1.** Properties of concentrated solutions of silica nanoparticles (NPs) in distilled water.

| Nanofluid (NF) | Basis | Modification | Concentration (wt.%) | Size (nm) |
|:---:|:---:|:---:|:---:|:---:|
| 1 | $SiO_2$ (sol–gel cationic) | Polymer | 38.6 | 107 |
| 2 | $SiO_2$ (sol–gel anionic) | Polymer | 26.0 | 32 |
| 3 | $SiO_2/Al_2O_3$/MOX | Polymer | 21.6 | 218 |
| 4 | $SiO_2/Al_2O_3$/MOX | Polymer | 25.5 | 145 |

Synthetic water was prepared under laboratory conditions, dissolving a certain amount of salts in distilled water to simulate the composition of the North Sea formation water (Table 2) of 38,318 ppm of total dissolved salts.

**Table 2.** Composition of synthetic sea water in a 1 L bottle.

| Salts | NaCl | KCl | NaHCO$_3$ | Na$_2$SO$_4$ | CaCl$_2$·6H$_2$O | MgCl$_2$·6H$_2$O | Sr$_2$·6H$_2$O |
|-------|------|-----|-----------|--------------|------------------|------------------|----------------|
| wt.% | 25.50 | 0.72 | 0.22 | 4.06 | 1.62 | 3.16 | 0.02 |

The measured density of water was 1.024 g/cm$^3$ and it had a viscosity of 1.025 cP. With added NPs to the injection seawater, the new density and viscosity were 1.023–1.028 g/cm$^3$, and 1.023 to 1.058 cP, respectively. This clearly shows a negligible effect of NPs on the initial properties of the injection water. It is worth mentioning that the properties were measured at room conditions ($\approx$21 °C) using an Anton Paar Density meter and Anton Paar Rheometer for density and viscosity, respectively. The pH of the water solution was 7.96, and with added NPs, a slight change was observed causing it to be between 7.53 and 8.10.

## 2.2. Crude Oil and Normal Decane

The crude oil was obtained from a field in the North Sea. Its viscosity was 33 cP and the gravity was 28° API at room conditions ($\approx$21 °C). The characterization of the degassed crude oil in terms of saturates, aromatics, resins, and asphaltenes (SARA) analysis is provided in Figure 1. It was a light crude oil with an asphaltenes content of 0.18 wt.%. Before use, the crude oil was filtered twice through a 5-$\mu$m Millipore to remove any suspended particles or other impurities that could affect its composition and flooding experiments [11]. The crude oil was used in oil recovery experiments. However, normal decane with a density of 0.73 g/cm$^3$ and viscosity of 0.92 cP at 20 °C was used for wettability tests.
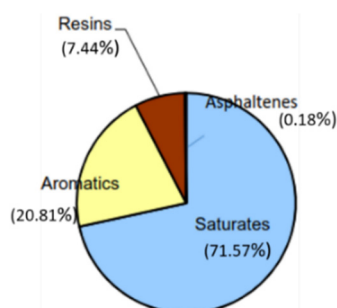


**Figure 1.** Saturates, aromatics, resins, and asphaltenes (SARA) analysis (wt.%) for crude oil.

## 2.3. Type of Porous Media

Oil recovery experiments were conducted using originally water-wet Berea sandstone rocks. The mineral composition of the rocks was characterized with X-ray diffraction (XRD) on five rock samples. The flooded core plugs were nearly homogeneous and composed of 93.7 vol.% quartz, 5.0 vol.% of microcline (alkali feldspar), and diopside (1.3 vol.%), on average. For flooding experiments, cylindrical core samples were prepared with standardized dimensions: diameter of 3.8 cm, and length varied from 4.5 to 6 cm. The cores were cleaned with methanol using Soxhlet extraction and dried in the oven at 60 °C for three days. Then, they were evacuated for 2 h and saturated with water using a vacuum container. The porosity was determined via a helium porosimeter and ranged from 16.7 to 19%. The core absolute permeability varied between 277 and 400 mD and was measured using a constant head permeameter with nitrogen gas and then corrected for the Klinkenberg effect.

## 2.4. Interfacial Tension Measurement

Interfacial tension (IFT) is an important parameter for oil recovery. It provides a qualitative measure of the movement and distribution of fluids in porous spaces. In this work, IFT was measured with the pendant drop technique. A J-syringe needle with an inner diameter of 1.0047 mm was sued to dose crude oil drops in the bulk phase. With the oil drop hanging from a needle within the continuous phase, IFT was measured every 20 s until equilibrium was reached. All measurements were carried out at room temperature.

## 2.5. Rock Wettability Tests

The wettability of a reservoir affects the location, the flow, and distribution of fluids in porous media [32]. Together with IFT, wettability plays a great role in all stages of oil recovery. The wettability of a reservoir can change during oil production process, as the polar crude oil substances adsorbed on the pores of the rock can be gradually desorbed. In petroleum engineering, the wettability of reservoir rocks is widely characterized by the Amott test. The test combines spontaneous and forced displacements of fluids to measure the average wetting condition of a reservoir rock [32]. In this work, the Amott test was used to assess the wettability of the core plugs before and after nanofluid injection. The spontaneous imbibition/drainage tests were performed using Amott cells: an Amott cell is a visual glass with a graduation tube on top [33]. For the spontaneous imbibition (SI) tests, an oil-saturated core plug was placed in an Amott cell filled with water. The oil displaced by water from the core was collected and read step by step through the graduation tube until equilibrium was reached. For the spontaneous drainage, the difference lies in the fact that a water-saturated core is placed in an oil-filled cell to measure the displacement of water by oil. At the end of each test, the forced displacement followed with the core plug being inserted in a Hassler core holder. The commonly used range of wettability indexes proposed by Cuiec [34] for the categorization of different rock wettability is shown Figure 2.
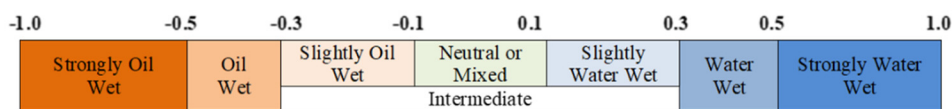


**Figure 2.** Categorization of rock wettability based on the wettability index.

## 2.6. Rock Core Flooding Experiments

Core flooding tests are widely used to study how well fluids can flow through porous media and oil recovery. The schematic diagram of the core flooding rig in Figure 3 shows the arrangement which was used in this work. The system consists of individual fluid-holding cylinders, containing crude oil, water, and nanofluid. All cylinders were mounted vertically inside a temperature-controlled oven. The core block consists of a Hassler-type core holder in which the core was loaded and oriented horizontally. The core block was supported by a customized stand, and the core was confined with an overburden pressure (confining pressure) held within 18–22 bars. The designated fluid was injected into the core at a time with the aid of a dual-pump continuous flow system, using hydraulic fluid. The fluid flow behavior through the pores was studied via pressure sensors connected to the inlet and outlet of the core holder, providing digital pressure drop acquisition data.
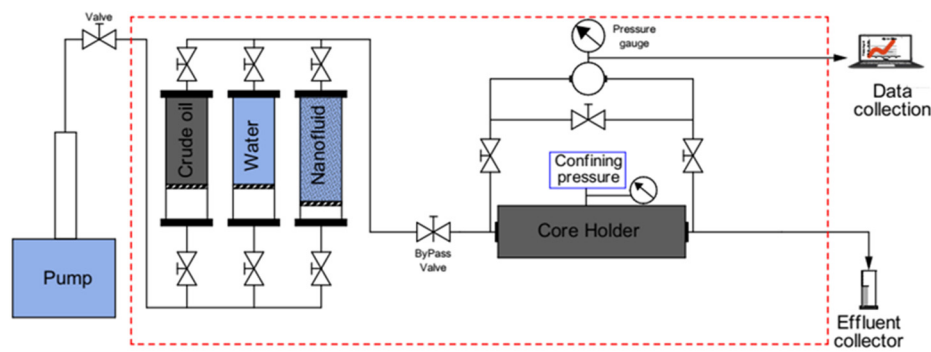
**Figure 3.** Schematic diagram of the core flooding system.

To simulate oil production of a reservoir: (i) initial water saturation ($S_{wi}$), was established by flooding the water-saturated core with crude oil at different flow rates (0.5, 1.5, and 3 mL/min), until there was no water production at the core outlet. This included flowing crude oil in both core ends to even the distribution of fluids. However, the sequential increase in flow rate was intended to reduce zones of capillary end-effects [35,36]. The original oil in place (OOIP) was measured as the volume of water displaced by the crude oil from the pores of the rock. Initial water saturation ($S_{wi}$) was calculated from the production $S_{wi} = (V_P - OOIP)/V_P \times 100\%$, (18.40–33.93%), while residual oil was determined at the end of oil recovery process. $V_P$ stands for the rock pore volume and was determined by the saturation method. (ii) As the next step, nanofluid was injected at a constant rate (0.2 mL/min) until there was no oil production for approximately 3 pore volumes (PVs), and this simulated the secondary oil recovery process (typically water flooding). Finally, (iii) in the tertiary oil recovery step, nanofluid was injected into the core to displace the waterflood residual oil saturation, using the same flow rate until there was no more oil production at the core outlet. The effluent was collected in 5 mL vials; an automated camera was used to record production during the slow oil production stage. All experiments were conducted at room conditions of temperature 21–23 °C and pressure 1 atm. To determine experimental repeatability and reduce errors, EOR tests were carried out on duplicate sets of nearly identical cores for each nanofluid type.

## 3. Results and Discussion

### 3.1. Nanoparticle Oil Recovery Performance

It is well known that, for most oil reservoirs, water flooding (WF) is the most preferred technique for maintaining reservoir pressure after primary depletion and for displacing a portion of the remaining oil to production wells. Availability of water, high recovery rates and low costs for execution make the WF technique the primary choice for oil companies [2,37,38]. However, injection chemical EOR fluids can mobilize mobile oil and residual oil, so they can be applied after the primary oil production stage, as a secondary recovery fluid. In this case, the displacement efficiency must be better than the water flooding [39]. A series of control experiments with injection water was carried out to verify this hypothesis in this work.

The results of sixteen core flood experiments proved the chemical EOR potential of silica-based nanofluids. As secondary EOR fluids, NPs showed potential to retard the breakthrough time compared to the plain water injection. Accordingly, higher ultimate recoveries were achieved by the nanofluid system than the injection of "pure" water. This is likely to happen because WF suffers from viscous fingering, causing an earlier water breakthrough and excessive water production and therefore poor sweep efficiency. Viscous fingering results from the displaced phase (crude oil) having higher viscosity than oil recovery displacing fluid [40]. Although the NPs did not show a tangible effect on the viscosity of injection water, the delayed water breakthrough time can be explained in terms of the structuring of NPs on the rock surface and subsequent plugging of some reservoir pore channels. As elucidated by Wang et al. [41], the existence of NPs, either attracting or repelling water molecules, changes the

pressure distribution of fluids, thus modifying the capillary and viscous forces. Accordingly, the water flow paths become more tortuous, delaying the breakthrough time [42]. In this work, the experiments were stopped after the injection of about 10 PVs of nanofluids, when there was no production. Under the experimental conditions, the injected PVs may be enough to support the long-range structuring of NPs within pores; this allowed the nanofluids to perform their designated physical–chemical interactions better, resulting in higher ultimate recovery than the reference waterflood. A comparison of the ultimate oil recoveries, for water and nanofluid flooding, as a function of injected pore volumes is given in Figure 4. The average (eight tests) recovery by waterflood was 39.7% ± 2.3 of the OOIP that varied from 35.1 to 43.1% (see Table 3). The oil displacement by nanofluids gave higher recoveries than the use of plain water. The recovery rates varied from 48 to 54.4% of the OOIP, and standard deviation was about 3% of the OOIP. This means that the nanofluids increased oil recovery by factors between 8.3 and 14.8%.
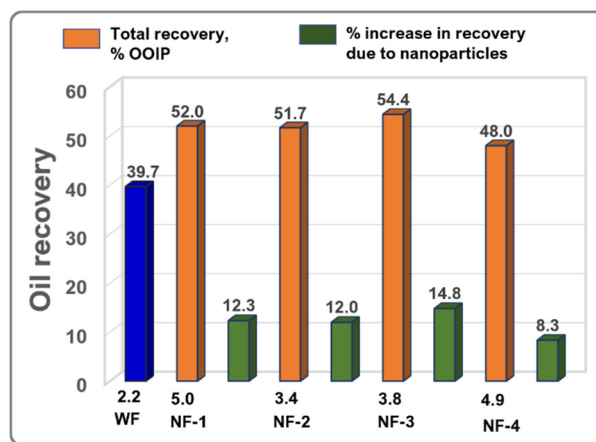


**Figure 4.** Secondary oil recoveries from various nanofluids compared to the reference waterflood. The numbers on the *X*-axis show average pore volumes injected to reach ultimate oil production.

The flood tests showed that oil can be produced to a certain extent nanofluids injection, after that, little or no oil is recovered even with prolonged injections time. This clearly indicated that NPs gradually became trapped in the thief zones and formed nano-layers, reducing reservoir permeability and becoming less efficient for recovery of oil. Therefore, it seems expedient to design a highly stable nanofluid solution with potency to trigger physical and chemical interactions as soon as possible, when in contact with the reservoir and its constituents. Due to the heterogeneous nature of most reservoirs, the nanofluid system must be designed with the characteristics of the specific oil field in mind. In addition, the optimal range of NPs concentration in the carrier fluid is recommended to be estimated based on likely recovery mechanisms for such an oil field to achieve a better oil sweep.

Additional eight tests were conducted with the same nanofluids in tertiary mode, at room conditions. In this case, 6 cm long cores were used. It was observed that for the nanofluid to mobilize residual oil and form a producible oil bank, a minimum of 1 PV injection was required. While most cores failed to mobilize residual oil to the core outlet at 1 PV, one core had a recovery of 3.3% of the OOIP with nanofluid (NF-1) injection. Probably, the core properties, PVs injected during the WF stage and oil accumulated at the core outlet due to the capillary end-effects can explain this deviation. Figure 5 presents the oil recovery profiles for selected samples. A summary of all recoveries from all nanofluids is given by Table 3.
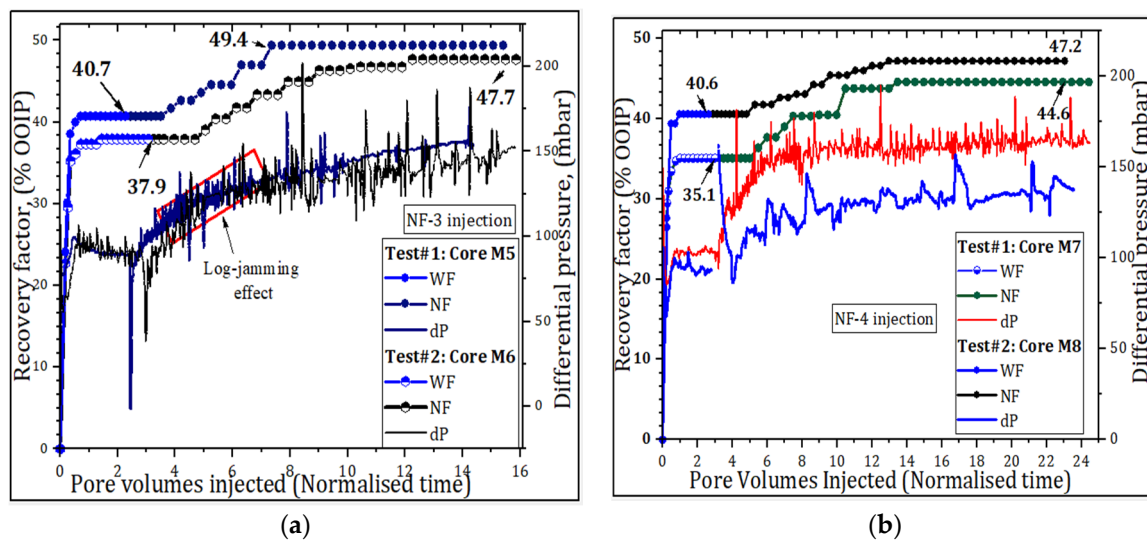
**Figure 5.** Influence of nanoparticles on oil recovery and on differential pressure: (**a**) water flood oil recovery in cores M5 and M6 was 40.7% and 35.9% OOIP, respectively; after nanofluid "NF-3", the recovery was 49.4% and 47.7% OOIP. (**b**) In cores M7 and M8, WF recoveries were 35.1% and 40.6% OOIP, respectively; after nanofluid "NF-4" injection, they increased to 44.6% and 47.2% OOIP, respectively.

**Table 3.** Oil recovery factors (expressed as % of the original oil in place (OOIP)) and residual oil saturation achieved at the end of core flood tests.

| NF | Core # | $V_P$ (mL) | $S_{wi}$ (%) | Water Flood | | Nanofluid Flood | | | $E_D$ (%) | Total RF (%) |
|---|---|---|---|---|---|---|---|---|---|---|
| | | | | RF (%) | $S_{or1}$ (%) | RF (%) | $\overline{RF}$ (%) | $S_{or2}$ (%) | | |
| NF-1 | M1 | 11.8 | 33.93 | 43.1 | 37.61 | 4.6 | 5.9 | 35.55 | 8.11 | 47.7 |
| | M2 | 12.0 | 24.22 | 38.9 | 46.29 | 7.3 | | 40.83 | 11.79 | 46.2 |
| NF-2 | M3 | 11.7 | 24.68 | 41.7 | 43.91 | 7.4 | 7.2 | 38.36 | 12.67 | 49.1 |
| | M4 | 12.2 | 20.68 | 39.4 | 48.05 | 7.0 | | 42.52 | 11.50 | 46.4 |
| NF-3 | M5 | 11.4 | 20.78 | 40.7 | 43.07 | 8.7 | 9.2 | 36.78 | 14.63 | 49.4 |
| | M6 | 11.1 | 20.73 | 37.9 | 49.22 | 9.8 | | 41.47 | 15.74 | 47.7 |
| NF-4 | M7 | 8.1 | 23.97 | 35.1 | 49.35 | 9.5 | 8.1 | 42.14 | 20.71 | 44.6 |
| | M8 | 8.3 | 18.40 | 40.6 | 48.48 | 6.6 | | 43.09 | 11.14 | 47.2 |
| | Average | | | 39.7 | 45.75 | | | 40.00 | | |

After the WF ceased production (for 2 to 4 PVs), the silica-based nanofluid, at a concentration of 0.1 wt.% ($\approx$10 PVs injected), increased the waterflood sweep efficiency. The average total recovery was 47.3% ($\pm$1.5) of the OOIP and varied from 44.6 to 49.4% of the OOIP. The displacement efficiency ($E_D$) varying in between 8.11% and 20.71% was evaluated by Equation (1). The $E_D$ and the decrease in residual oil saturation (see Table 3) prove that silica NPs can improve sweep efficiency at a microscopic level.

$$E_D = \left[1 - \left(\frac{S_{or2}}{S_{or1}}\right)\right] \times 100\% \tag{1}$$

Here, $S_{or1}$ and $S_{or2}$ represent residual oil saturation after water flooding and nanofluid flooding, respectively. Residual oil saturation was evaluated as follows:

$$S_{or} = \left(\frac{OOIP - N_P}{V_P}\right) \times 100\% \tag{2}$$

where, $N_P$ is the cumulative oil production at the end of the flooding operation.

The average incremental recovery varied between 5.9% and 9.2% of the OOIP with a maximum standard deviation of 2% of the OOIP. Inspection of the results presented in Figure 4 and Table 3 shows high total recoveries in secondary recovery mode compared with tertiary mode. The results support the notion that, for practical applications, NPs are preferable/efficient as secondary EOR fluids. Similar results were reported by Torsater et al. [43]. Moreover, in tertiary mode, many pore volumes of nanofluids are needed to increase the recovery factor compared to secondary injection. In this regard, tertiary operation may also raise concerns about the cost of nanomaterials. In addition to the surface activity of the NPs, the nanofluid recovery potential depends mainly on the time-dependent physical–chemical interactions with the rock system. For instance, the gradual increase in oil recovery seen in Figure 5, in the nanofluid injection stage, evidences the effect of the long-range structural disjoining pressure mechanism in enhancing oil recovery. The longer the time the nanofluids are in contact with the rock system, the better the oil recovery [44]. In summary, the polymer-coated silica NPs revealed a good EOR potential in water-wet rocks. Additional flood tests are recommended at conditions of high temperature and high pressure to best mimic oil field conditions. This should include the application of a bump flood at the end of a low-rate injection to mitigate the capillary end-effects and to ensure that the waterflood residual oil saturation has been established prior to the implementation of the EOR fluid injection.

### 3.2. Evaluation of Nanoparticle Oil Recovery Mechanisms

### 3.2.1. Interfacial Tension Analysis

The interfacial tension (IFT) between the aqueous solution of NPs and crude oil phases was evaluated at room conditions with the pendant drop method. Figure 6a shows the dynamic measurement of the IFT versus time. The reference tension (crude oil/water) was 10.6 mN/m [17]. As shown in Figure 6a, this tension was reduced to a range of 6.8–4.1 mN/m by the NPs in the aqueous phase. Figure 6b also demonstrates that the reduction in IFT is, in part, dependent on particle size, in agreement with earlier studies [19,20]. The nanoparticles' size was measured with the dynamic light scattering method. Binks [45] emphasized that if the coating of particles is homogeneous over the particle surface, such particles are surface-active. Accordingly, the particles will have a very high energy of attachment to the interfaces, that is, NPs will adsorb irreversibly to the interfaces [45]. Such irreversible attachment, as discussed by Binks [45], is observed in particles of size greater than 0.5 nm (radius) as those studied in this work. The strong attachment allows the particles to effectively contact a large surface area at the interface and decrease the oil/water tension and stabilize oil drops in aqueous phase. However, as the particle coverage at the interface approaches a maximum, the presence of already attached particles may hinder further adsorption of particles [46]. Behera and Sangwai [47] explain that NPs tend to increase repulsive forces within them, inducing a higher disjoining pressure, which is responsible for the reduction in IFT between the two phases. Besides, this phenomenon can be, in part, attributed to the surface-active polymer shells bonded to the NP surface, intended to enhance steric repulsive forces and stabilization of NPs. Understanding the role of surface-active particles, i.e., particle and particle surface-coating agents, in reducing the tension and therefore in mobilizing residual oil remains an issue. Physico-chemical interactions as a result of the bonding of silica NPs with surface-coated polymers, such as improved surface reactivity and stability, are likely to play a role in reducing IFT and therefore in the efficient displacement of oil at a microscopic level. A reduction in IFT, even below the critical value for the onset of oil mobilization, is regarded crucial for oil recovery, as it can change the microscopic distribution of the oil in porous spaces [48]. Additionally, polymer-coated NPs can stabilize oil droplet emulsions [49], paving the way for their efficient mobilization towards production wells and increased oil recovery. We confirmed experimentally that nanofluids NF-1 and NF-2 could generate oil–water emulsions by increasing the injection rate at the end of a low-rate injection. Potentially, oil was recovered as an emulsion in water phase. This observation is well related to its small size and the ability to reduce IFT compared to samples NF-3 and NF-4, which did not share

the same behavior. It has also been claimed that NPs' emulsification ability is, in part, attributed to the surface activity of the polymer molecules [13]; the polymer molecules can enter the oil/water interface and decrease surface energy and interfacial tension.
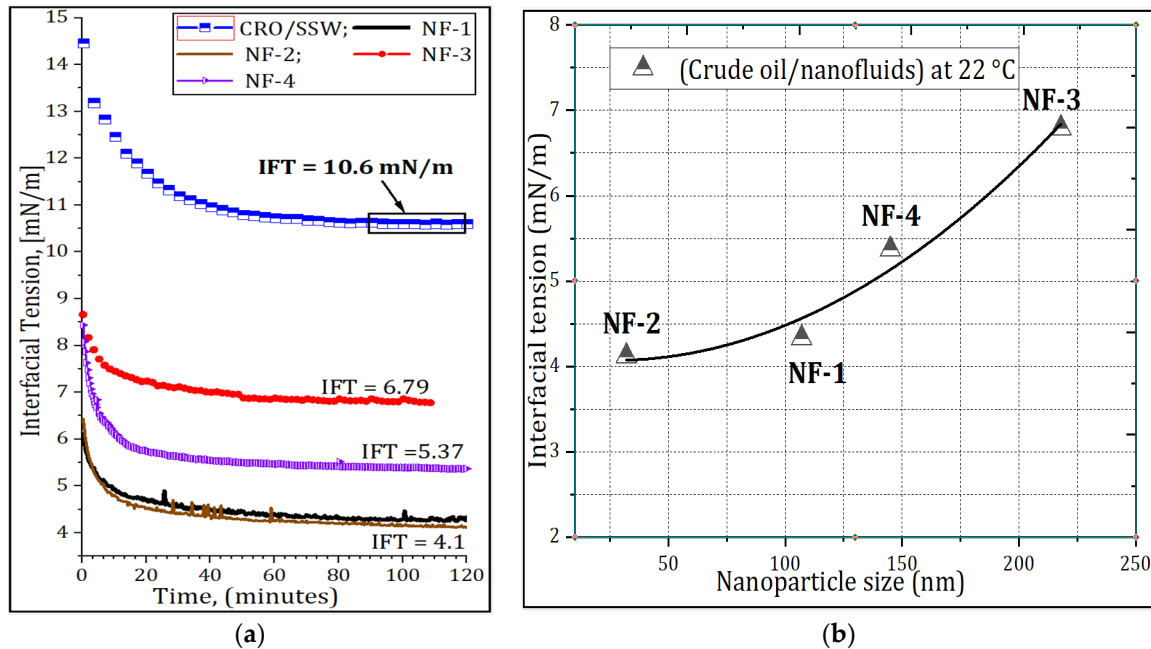


**Figure 6.** (**a**) Dynamic measurement of interfacial tension (IFT) between crude oil (CRO) and nanofluids, and (**b**) variation of IFT with nanoparticles' size.

Although there is a correlation between IFT reduction and the size of the NPs, the same does not apply for oil recovery. For instance, NF-2, with the smallest particle size and therefore the largest IFT reduction (4.1 mN/m), had an incremental recovery of 7.2% of the OOIP, while the largest particle size sample, NF-3, with the highest IFT value, recorded the highest incremental recovery of 9.2% of the OOIP. As the IFT does not change dramatically when adding polymer-coated silica NPs to water, it is therefore not a primary mechanism responsible for the EOR effect. We speculate that the surface-coating polymers' molecules left insufficient accessible surface sites for the NPs adsorption, thus impending them to play their role at the interfaces. Further studies should be conducted in order to determine the ideal conditions for NP surface coating to achieve the lowest IFT and, at the same time, be efficient in providing high stability for NP dispersion during the EOR operation.

### 3.2.2. Spontaneous Imbibition Tests

Having examined the influence of NPs on fluid properties in Section 3.2.1, next, we studied how the nanoparticles could affect the rock surface property and oil recovery during nanofluid flooding oil recovery process. The wettability alteration was measured with cores after nanofluid displacement by a spontaneous imbibition (SI) test at room temperature for a period of time. Oil production curves and imbibition rates were used to realize the nanoparticle EOR mechanisms. The core with residual crude oil was saturated with decane and placed in a water-filled Amott cell. The volume of oil produced by spontaneous imbibition is plotted against the time in Figure 7. The upper curve shows the highest imbibition rate and the highest cumulative oil production achieved by the reference or original core, that is, not contacted by the nanoparticles. The cores treated by the NPs seem to follow the same oil recovery profile (at early stages of SI) to a point where the imbibition rate decreases, and the oil production stops momentarily. Meanwhile, original core water continued to imbibe, and increased oil recovery, indicating a strongly water-wet nature of the rocks before oil recovery tests. A gradual increase in oil production after a stagnant period can be seen in cores contacted by nanoparticles.

This shows that the polar components of the crude oil were desorbed during the nanoparticle EOR process and the residual oil decreased, improving the oil sweep efficiency. Moreover, as the NPs stayed longer in contact with the rock, water could gradually imbibe owing to the dynamic alteration in the rock wettability to being more water-wet induced by NP interactions.
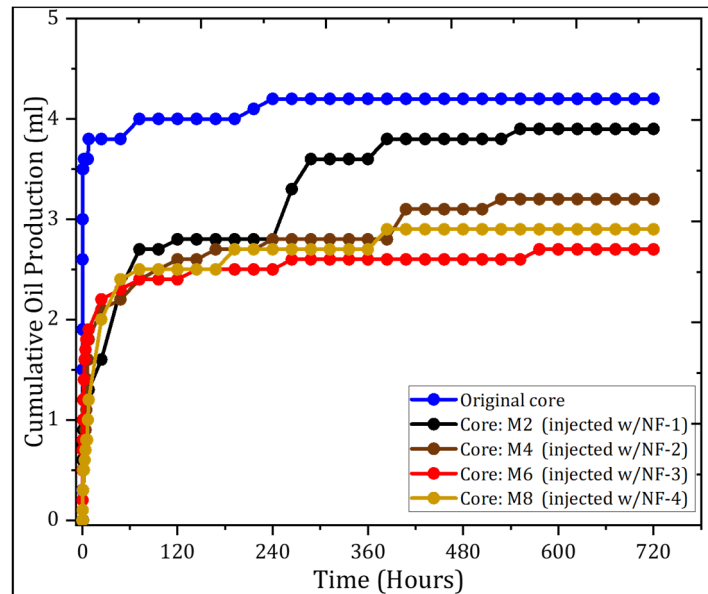


**Figure 7.** Oil recovery by spontaneous imbibition versus time.

The cumulative oil production seems inversely related to the IFT reduction and the nanoparticle size. In other words, the core plugs injected with small-size NPs exhibited a better capillary water intake and high recovery by SI, in agreement with the results obtained in Figure 6b. The Amott water index ($I_W$) varied from 0.54 to 0.78; the wettability index from the reference core plug was measured in our previous work and was 0.86 [30]. The rate of SI and $I_W$ indicates a wettability alteration to a more water-wet state due to the injected hydrophilic nanoparticles. In the absence of attractive forces between the NPs and rock surface, Wasan and Nikolov [26] and Chengara et al. [27] explain that the layering and structuring arrangement of NPs in the pores causes the disjoining pressure, which attempts to separate crude oil from the rock surface; accordingly, this reduces residual oil and improves the recovery of oil. However, the variation in core wettability by hydrophilic NPs seems minimal to fully account for a significant oil recovery. To eliminate this ambiguity, further research is recommended to check for possible changes in the wettability after the water flooding stage. Then, a solid interpretation can be drawn on the ability of NPs to induce tangible changes in the wettability.

3.2.3. Transport Behavior of Nanoparticles during EOR Process

The existence of NPs, either attracting or repelling water molecules, can change the pressure distribution of fluids; this can modify the capillary and viscous forces, resulting in different displacement velocity and sweep efficiency [41]. Hence, careful analysis of the differential pressure during core floods can provide useful data for interpreting the transport of NPs through pore channels and, therefore, nanoparticle oil displacement mechanisms.

For any of the flooding modes, the pressure increased with the injection of nanofluid and was higher than the reference waterflood pressure. Examples of pressure profiles for water flooding (WF) followed by nanofluid flooding are presented in Figure 5. In the WF stage, the pressure stabilizes after the breakthrough point, because the oil ceased production. Then, the pressure increases with the injection of nanofluid; however, little or no entrainment of oil occurred at this stage. With the progress of the injection, the particles caused pressure fluctuations. Long periods of spiky pressure were noticeable during the injection of samples NF-3 and NF-4, probably due to their larger particle size.

The fluctuations in pressure indicate blockage of some pore channels followed by pore-opening and mobilization of residual oil [42]. The square in Figure 5 shows the log-jamming effect and subsequent obstruction of some pore channels. The pressure curves show a slow pore blocking process to a point where maximum blockage is achieved, creating excess local pore pressure. To search for new flow paths and relieve the excess inner pore pressure in the particle jammed zones, the pressure had to be redistributed between the adjacent pores; this allowed the injection water to be (re)directed to unswept zones. Furthermore, the areas of sudden increased pressure (in Figure 5) may reflect in oil droplets squeezed in the constricted pores, followed by breakage, and therefore allowing the release of pressure and oil entrainment [42]. This process facilitates the recovery of oil at a microscopic level [28,29]. Table 3 shows high oil displacement efficiency from larger size particles. In Section 3.2.1, it was noted that large-size NPs had the least influence on the IFT reduction. Hence, the interpretation of the pressure profile suggests that not only the log-jamming effect but also straining occurred during oil mobilization process. It was observed that the pressure increase was significant during the injection of the nanofluid in the secondary mode compared to the tertiary mode. This can be attributed to the displacement of the viscous oil saturated core and subsequent entrapment of oil ganglia in narrow pore throats, along with physical confinement of nanoparticles. In contrast, waterflood residual oil saturation is found in the smaller pores, as a continuous film on the surface, and as larger pockets trapped by water, and can be produced at low pressure drops [32]. Moreover, during waterflood water tends to establish flow routes through which the NPs can pass through at later stage of the injection, which can minimize the pressure drop.

The reduction in core permeability varied from 7 to 24% of initial values and can be explained by either irreversible retention or agglomeration of NPs in the pores. The largest reduction in initial core permeability was found in those injected with large-size particles. However, the observed pressure variance reflects small changes in the permeability of the cores. This implies that the polymer molecules attached to the particle's surface played some role in improving the transport of NPs through Berea sandstone pores while facilitating the recovery of oil.

When carrying out nanoparticle EOR experiments in a constant flow, determining the contribution of pressure increase in oil mobilization remains a challenge. This is because the pressure is unstable even if there is no more oil recovery. For practical applications, it seems relevant to conduct the displacement of oil with NPs in the reservoir under a constant pressure drop. In order to realize different physical processes of the NPs' displacement mechanisms, further research is recommended to perform recovery tests with nanoparticles at a constant pressure drop. Our expectations are that the total volumetric rate will decrease over time because NPs will result in the log-jamming effect and reduce permeability. The jamming effect, wetting change and low IFT can still increase the rate of oil production to some extent, although the overall rate is reduced.

## 4. Conclusions

This paper reports on the potential application of silica-based nanofluids for oil recovery, as well as the underlying oil recovery mechanisms. The results showed that NPs at a concentration of 0.1 wt.% in seawater can increment oil recovery in water-wet reservoirs. Different mechanisms, such as IFT reduction, modification of the surface roughness due to structuring of nanoparticles in the rock pores and wettability variation to more water-wet, and the log-jamming effect can explain the silica-based nanoparticle EOR effect in water-wet reservoirs. Additional findings include:

- The NPs at 0.1 wt.% had a minor effect on the viscosity of the injection water; however, they showed an ability to retard the breakthrough time, resulting in a high recovery compared to the base case (waterflood).
- Hydrophilic silica nanoparticles (polymer-coated $SO_2$) seemed to be more effective in enhancing oil recovery as secondary EOR fluids in Berea sandstone.
- Hydrophilic silica nanoparticles are capable of gradually changing the microscopic distribution of fluids due to deposition on the rock surface, changes in the surface roughness and wettability of

the rock to a more water-wet condition, which could be an important mechanism for long injection periods expected at a field scale.

- Generation of in situ oil emulsion droplets in water phase could be an influencing factor on the recovery of oil for some small-size nanoparticles.

## References

1. Sun, X.; Zhang, Y.; Chen, G.; Gai, Z. Application of Nanoparticles in Enhanced Oil Recovery: A Critical Review of Recent Progress. *Energies* **2017**, *10*, 45. [CrossRef]

2. Muggeridge, A.; Cockin, A.; Webb, K.; Frampton, H.; Collins, I.; Moulds, T.; Salino, P. Recovery rates, enhanced oil recovery and technological limits. *Philos. Trans. Ser. A Math. Phys. Eng. Sci.* **2014**, *372*, 2006. [CrossRef]

3. Sandeep, R.; Jain, S.; Agrawal, A. Application of Nanoparticles-Based Technologies in the Oil and Gas Industry. In *Nanotechnology for Energy and Environmental Engineering*; Springer: Berlin/Heidelberg, Germany, 2020; pp. 257–277.

4. Ahmadi, M.; Habibi, A.; Pourafshari, P.; Ayatollahi, S. Zeta Potential Investigation and Mathematical Modeling of Nanoparticles Deposited on the Rock Surface to Reduce Fine Migration. In *SPE Middle East Oil and Gas Show and Conference*; Society of Petroleum Engineers: Manama, Bahrain, 2011; p. 14.

5. Bennetzen, M.V.; Mogensen, K. Novel Applications of Nanoparticles for Future Enhanced Oil Recovery. In *International Petroleum Technology Conference*; International Petroleum Technology Conference: Kuala Lumpur, Malaysia, 2014; p. 14.

6. Negin, C.; Ali, S.; Xie, Q. Application of nanotechnology for enhancing oil recovery—A review. *Petroleum* **2016**, *2*, 324–333. [CrossRef]

7. Miranda, C.R.; Lara, L.S.d.; Tonetto, B.C. Stability and Mobility of Functionalized Silica Nanoparticles for Enhanced Oil Recovery Applications. In *SPE International Oilfield Nanotechnology Conference and Exhibition*; Society of Petroleum Engineers: Noordwijk, The Netherlands, 2012; p. 11.

8. Bera, A.; Belhaj, H. Application of nanotechnology by means of nanoparticles and nanodispersions in oil recovery-A comprehensive review. *J. Nat. Gas Sci. Eng.* **2016**, *34*, 1284–1309.

9. Ding, H.; Zhang, N.; Zhang, Y.; Wei, M.; Bai, B. Experimental Data Analysis of Nanoparticles for Enhanced Oil Recovery. *Ind. Eng. Chem. Res.* **2019**, *58*, 12438–12450. [CrossRef]

10. Zhou, Y.; Wu, X.; Zhong, X.; Reagen, S.; Zhang, S.; Sun, W.; Pu, H.; Zhao, J.X. Polymer nanoparticles based nano-fluid for enhanced oil recovery at harsh formation conditions. *Fuel* **2020**, *267*, 117251. [CrossRef]

11. Bila, A.L. Experimental Investigation of Surface-Functionalised Silica Nanoparticles for Enhanced Oil Recovery. Ph.D. Thesis, Norwegian University of Science and Technology (NTNU), Trondheim, Norway, 2020.

12. Omran, M.; Akarri, S.; Torsaeter, O. The Effect of Wettability and Flow Rate on Oil Displacement Using Polymer-Coated Silica Nanoparticles: A Microfluidic Study. *Processes* **2020**, *8*, 991. [CrossRef]

13. Saigal, T.; Dong, H.; Matyjaszewski, K.; Tilton, R.D. Pickering emulsions stabilized by nanoparticles with thermally responsive grafted polymer brushes. *Langmuir* **2010**, *26*, 15200–15209. [CrossRef]

14. Qi, L.; Song, C.; Wang, T.; Li, Q.; Hirasaki, G.J.; Verduzco, R. Polymer-coated nanoparticles for reversible emulsification and recovery of heavy oil. *Langmuir* **2018**, *34*, 6522–6528. [CrossRef]

15. Ponnapati, R.; Karazincir, O.; Dao, E.; Ng, R.; Mohanty, K.K.; Krishnamoorti, R. Polymer-functionalized nanoparticles for improving waterflood sweep efficiency: Characterization and transport properties. *Ind. Eng. Chem. Res.* **2011**, *50*, 13030–13036. [CrossRef]

16. Bila, A.; Stensen, Å.J.; Torsæter, O. Polymer-functionalized silica nanoparticles for improving water flood sweep efficiency in Berea sandstones. *E3s Web Conf.* **2020**, *146*, 02001. [CrossRef]

17. Bila, A.; Stensen, Å.J.; Torsæter, O. Experimental Investigation of Polymer-Coated Silica Nanoparticles for Enhanced Oil Recovery. *Nanomaterials* **2019**, *9*, 882. [CrossRef] [PubMed]

18. Aziz, H.; Tunio, S.Q. Enhancing oil recovery using nanoparticles—A review. *Adv. Nat. Sci. Nanosci. Nanotechnol.* **2019**, *10*, 033001. [CrossRef]

19. Tangparitkul, S.; Charpentier, T.V.J.; Pradilla, D.; Harbottle, D. Interfacial and colloidal forces governing oil droplet displacement: Implications for enhanced oil recovery. *Colloids Interfaces* **2018**, *2*, 30. [CrossRef]

20. Chevalier, Y.; Bolzinger, M.-A. Emulsions stabilized with solid nanoparticles: Pickering emulsions. *Colloids Surf. A Physicochem. Eng. Asp.* **2013**, *439*, 23–34. [CrossRef]

21. Afolabi, R.O.; Yusuf, E.O. Nanotechnology and global energy demand: Challenges and prospects for a paradigm shift in the oil and gas industry. *J. Pet. Explor. Prod. Technol.* **2019**, *9*, 1423–1441. [CrossRef]

22. Roustaei, A.; Saffarzadeh, S.; Mohammadi, M. An evaluation of modified silica nanoparticles' efficiency in enhancing oil recovery of light and intermediate oil reservoirs. *Egypt. J. Pet.* **2013**, *22*, 427–433. [CrossRef]

23. Zhang, T.; Davidson, D.; Bryant, S.L.; Huh, C. Nanoparticle-Stabilized Emulsions for Applications in Enhanced Oil Recovery. In *SPE Improved Oil Recovery Symposium*; Society of Petroleum Engineers: Tulsa, OK, USA, 2010; p. 18.

24. Adil, M.; Lee, K.; Zaid, H.M.; Latiff, N.R.A.; Alnarabiji, M.S. Experimental study on electromagnetic-assisted ZnO nanofluid flooding for enhanced oil recovery (EOR). *PLoS ONE* **2018**, *13*, e0193518. [CrossRef]

25. Kim, I.; Worthen, A.J.; Johnston, K.P.; DiCarlo, D.A.; Huh, C. Size-dependent properties of silica nanoparticles for Pickering stabilization of emulsions and foams. *J. Nanopart. Res.* **2016**, *18*, 82. [CrossRef]

26. Wasan, D.T.; Nikolov, A.D. Spreading of nanofluids on solids. *Nature* **2003**, *423*, 156–159. [CrossRef]

27. Chengara, A.; Nikolov, A.D.; Wasan, D.T.; Trokhymchuk, A.; Henderson, D. Spreading of nanofluids driven by the structural disjoining pressure gradient. *J. Colloid Interface Sci.* **2004**, *280*, 192–201. [CrossRef] [PubMed]

28. Spildo, K.; Skauge, A.; Aarra, M.G.; Tweheyo, M.T. A New Polymer Application for North Sea Reservoirs. *SPE Reserv. Eval. Eng.* **2009**, *12*, 427–432. [CrossRef]

29. Skauge, T.; Spildo, K.; Skauge, A. Nano-sized Particles For EOR. In *SPE Improved Oil Recovery Symposium*; Society of Petroleum Engineers: Tulsa, OK, USA, 2010; p. 10.

30. Bila, A.; Stensen, J.Å.; Torsæter, O. Experimental Evaluation of Oil Recovery Mechanisms Using a Variety of Surface-Modified Silica Nanoparticles in the Injection Water. In *SPE Norway One Day Seminar*; Society of Petroleum Engineers: Bergen, Norway, 2019; p. 19.

31. Kokubun, M.A.E.; Radu, F.A.; Keilegavlen, E.; Kumar, K.; Spildo, K. Transport of Polymer Particles in Oil–Water Flow in Porous Media: Enhancing Oil Recovery. *Transp. Porous Media* **2019**, *126*, 501–519. [CrossRef]

32. Anderson, W.G. Wettability Literature Survey Part 5: The Effects of Wettability on Relative Permeability. *J. Pet. Technol.* **1987**, *39*, 1453–1468. [CrossRef]

33. Nazari Moghaddam, R.; Bahramian, A.; Fakhroueian, Z.; Karimi, A.; Arya, S. Comparative Study of Using Nanoparticles for Enhanced Oil Recovery: Wettability Alteration of Carbonate Rocks. *Energy Fuels* **2015**, *29*, 2111–2119. [CrossRef]

34. Cuiec, L. Rock/Crude-Oil Interactions and Wettability: An Attempt To Understand Their Interrelation. In *SPE Annual Technical Conference and Exhibition*; Society of Petroleum Engineers: Houston, TX, USA, 1984; p. 14.

35. Ramakrishnan, T.S.; Cappiello, A. A new technique to measure static and dynamic properties of a partially saturated porous medium. *Chem. Eng. Sci.* **1991**, *46*, 1157–1163. [CrossRef]

36. Heaviside, J.; Black, C.J.J. Fundamentals of Relative Permeability: Experimental and Theoretical Considerations. In *SPE Annual Technical Conference and Exhibition*; Society of Petroleum Engineers: San Francisco, CA, USA, 1983; p. 17.

37. Youssif, M.I.; El-Maghraby, R.M.; Saleh, S.M.; Elgibaly, A. Silica nanofluid flooding for enhanced oil recovery in sandstone rocks. *Egypt. J. Pet.* **2018**, *27*, 105–110. [CrossRef]

38. Satter, A.; Iqbal, G.M. 7-Reservoir Life Cycle and Role of Industry Professionals. In *Reservoir Engineering*; Gulf Professional Publishing: Boston, MA, USA, 2016; pp. 127–136.

39. Green, D.W.; Willhite, G.P. *Enhanced Oil Recovery*; Henry, L., Ed.; Doherty Memorial Fund of AIME; Society of Petroleum Engineers: Houston, TX, USA, 1998; Volume 6.

40. Sydansk, R.D.; Romero-Zeron, L. *Reservoir Conformance Improvement*; Society of Petroleum Engineers Richardson: Houston, TX, USA, 2011.

41. Wang, X.; Xiao, S.; Zhang, Z.; He, J. Displacement of nanofluids in silica nanopores: Influenced by wettability of nanoparticles and oil components. *Environ. Sci. Nano* **2018**, *5*, 2641–2650. [CrossRef]

42. Rezaei, N.; Firoozabadi, A. Macro-and Microscale Waterflooding Performances of Crudes which form w/o Emulsions upon Mixing with Brines. *Energy Fuels* **2014**, *28*, 2092–2103. [CrossRef]

43. Torsater, O.; Engeset, B.; Hendraningrat, L.; Suwarno, S. Improved Oil Recovery by Nanofluids Flooding: An Experimental Study. In *SPE Kuwait International Petroleum Conference and Exhibition*; Society of Petroleum Engineers: Kuwait City, Kuwait, 2012; p. 9.

44. Zhang, H.; Ramakrishnan, T.S.; Nikolov, A.; Wasan, D. Enhanced oil recovery driven by nanofilm structural disjoining pressure: Flooding experiments and microvisualization. *Energy Fuels* **2016**, *30*, 2771–2779. [CrossRef]

45. Binks, B.P. Particles as surfactants—Similarities and differences. *Curr. Opin. Colloid Interface Sci.* **2002**, *7*, 21–41. [CrossRef]

46. Bizmark, N.; Ioannidis, M.A.; Henneke, D.E. Irreversible adsorption-driven assembly of nanoparticles at fluid interfaces revealed by a dynamic surface tension probe. *Langmuir* **2014**, *30*, 710–717. [CrossRef] [PubMed]

47. Behera, U.S.; Sangwai, J.S. Interaction of Nanoparticles with Reservoir Fluids and Rocks for Enhanced Oil Recovery. In *Nanotechnology for Energy and Environmental Engineering*; Springer: Berlin/Heidelberg, Germany, 2020; pp. 299–328.

48. Chatzis, I.; Kuntamukkula, M.S.; Morrow, N.R. Effect of capillary number on the microstructure of residual oil in strongly water-wet sandstones. *SPE Reserv. Eng.* **1988**, *3*, 902–912. [CrossRef]

49. ShamsiJazeyi, H.; Miller, C.A.; Wong, M.S.; Tour, J.M.; Verduzco, R. Polymer-coated nanoparticles for enhanced oil recovery. *J. Appl. Polym. Sci.* **2014**, *131*, 15. [CrossRef]

**Publisher's Note:** MDPI stays neutral with regard to jurisdictional claims in published maps and institutional affiliations.